Dynamic Glass Transition above the Cooperativity Onset in Poly(*n*-octyl methacrylate)

M. Beiner, J. Korus, and E. Donth*

Universität Halle, Fachbereich Physik, D-06099 Halle (Saale), Germany

Received November 19, 1996; Revised Manuscript Received June 20, 1997[⊗]

ABSTRACT: Experimental heat capacity, dielectric, and shear spectroscopy data are reported on the $\alpha\beta$ splitting region of poly(*n*-octyl methacrylate). New facets of a major difference between the high-temperature *a* relaxation at frequencies above the $\alpha\beta$ splitting region and the ordinary α relaxation below are obtained: An α cooperativity onset in the splitting region and dominance of Rouse−Zimm-like modes *R* for the *a* relaxation. The α and *a* relaxations are not related by temperature−time superposition.

I. Introduction

The dynamic glass transition at high frequencies is sometimes not only of academic but also of direct technological interest. For example, the wet skid resistance of tires is proportional to the mechanical loss at about 10^5 Hz[1] (resulting from the car velocity divided by the road roughness), i.e., far above T_g, and the adhesion and ultimative strength of rubber tearing are affected by properties of the main transition in the 10^9 Hz range. The properties at such high frequencies are usually estimated from the glass transition properties in the millihertz-to-kilohertz region by using temperature−time superposition, e.g., shifting the properties with a WLF curve. A detailed analysis of dynamic shear data at low and moderate frequencies shows that the main transition in polymers is thermorheologically complex and is characterized by two fine structure components[2−4] with encroachment.[5] Typical shear exponents are $s \equiv \mathrm{d}\log G'/\mathrm{d}\log\omega \approx 0.8...1.4$ ($\log = \log_{10}$), much larger than for Rouse modes.

On the other hand, dynamic neutron scattering proved unambiguously[6] that at high frequencies $\geq 10^8$ Hz and appropriate space resolution the main transition for several polymers can be described by Rouse modes *R* or Rouse−Zimm modes ($s = 0.5$ or 0.67), hindered at larger lengths by the entanglements. It is therefore not possible to get a reasonable description for high frequencies from the shift.

There are further arguments to assume that the character of the high-temperature relaxation *a* (sometimes also called $\alpha\beta$ relaxation) is qualitatively different from that of both the ordinary α (dynamic glass transition) and the β relaxation (Goldstein−Johari mode) below the $\alpha\beta$ splitting region *S* (Figure 1): (i) In a series of poly(*n*-alkyl methacrylate)s and random copolymers of the butyl member with styrene, the ΔC_p step tends to zero in the $\alpha\beta$ splitting region *S*.[7,8] This is interpreted as a *cooperativity onset* (index *on*) of the α glass transition in the $\alpha\beta$ splitting region of these polymers. (ii) The temperature dependence of the dielectric peak shape parameters and the α and β relaxation intensities significantly change in the splitting region for the polymers mentioned above,[9] for epoxy resins,[10,11] and for polybutadiene.[12] In particular, the dielectric intensity of the α component $\Delta\epsilon_\alpha = \Delta\epsilon - \Delta\epsilon_\beta$ tends linearly to zero in the splitting region. (iii) In a number of small molecule and polymeric glass formers, the WLF parameters of the main transition significantly change at a temperature T_B.[13−15] This change from one set of WLF parameters to another one is obviously connected with the $\alpha\beta$ splitting region.[16]

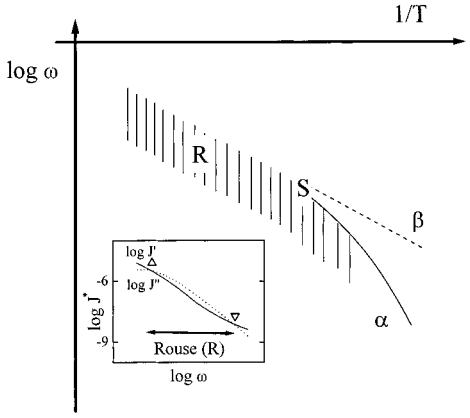

Figure 1. Schematical relaxation chart for polymers. Only the main transition α, the local mode β, the Rouse region *R*, and the $\alpha\beta$ splitting region *S* are shown. It is the proposition of this paper that the *a* process (see text) above *S* is dominated by *R*. The inset shows how the upper (∇) and lower ($\triangle$) frequency limit of the Rouse region were determined from the intersection of the J' and J'' shear compliance curves. The cooperativity onset is in the *S* region.

Heat capacity spectroscopy HCS[17] tests entropy fluctuations in the sample. In contrast to dielectric and shear spectroscopy, HCS is usually sensitive only to the α relaxation and not to the local β relaxation. The step of heat capacity, ΔC_p, is considered as an indicator for the α glass transition cooperativity. We expect, therefore, changes in the HCS signal if there are changes in the molecular cooperativity in the $\alpha\beta$ splitting region *S*.

The aim of this paper is to combine experimental data of shear, heat capacity, and dielectric spectroscopy in the $\alpha\beta$ splitting region of poly(*n*-octyl methacrylate) PnOMA. Since the $\alpha\beta$ splitting region of PnOMA is in the kilohertz range, i.e., accessible for all the three methods, we expect to observe real differences between the *a*, α, and β relaxations.

II. Experimental Section

The poly(*n*-octyl methacrylate) sample was synthesized by Dr. Th. Wagner from MPI-P Mainz. The average molecular weight, $\bar{M}_w$, is 154k with a polydispersity, $\bar{M}_w/\bar{M}_n$, of 2.2 determined by size exclusion chromatography with PMMA standards. The PnOMA sample was predried for 24 h at 80 °C under vacuum to remove solvable components and finally dried for 4 h at 80 °C under vacuum immediately prior to the

[⊗] Abstract published in *Advance ACS Abstracts,* December 15, 1997.

S0024-9297(96)01704-4 CCC: $14.00

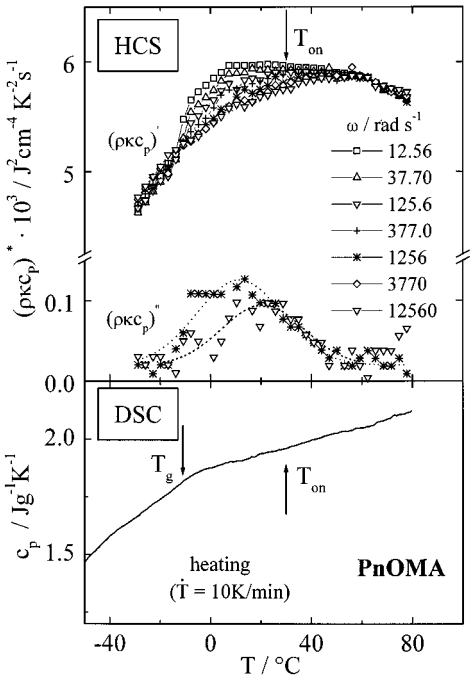

Figure 2. HCS $(\rho\kappa C_p)^*$ isochrones (top) and heat capacity C_p from DSC (bottom) versus temperature for poly(*n*-octyl methacrylate). The HCS onset temperature T_{on} and DSC glass transition temperature T_g are indicated by arrows.

measurements. The glass temperature $T_g = -11$ °C, as obtained by an equal area construction from a DSC heating run at 10 K/min (DSC7 instrument from Perkin-Elmer). The dielectric measurements were performed in a commercial Novocontrol dielectric spectrometer based on a Schlumberger FRA1260 signal analyzer. The sample had a thickness of about 100 μm and a diameter of 20 mm. A strain-controlled RDA II instrument from Rheometric Scientific was used for dynamic linear shear experiments in the temperature range from −25 °C to 20 °C with stripe geometry of about 1.5 × 10 × 20 mm^3. Additionally, the dynamic shear compliance in the temperature range from 25 to 55 °C was directly measured by a torque-controlled DSR instrument from Rheometric Scientific with parallel plates of 25 mm diameter and a sample thickness of about 0.7 mm. The combination of both shear instruments covered a frequency range of more than 5 decades, from $\omega = 1 \times 10^{-3}$ to 5×10^2 rad/s. The dynamic heat capacity in the frequency range from 12 to 1.2×10^4 rad/s was determined by an improved heat capacity spectrometer HCS using the 3ω method.[17] The details including the $(\rho\kappa C_p)^* \rightarrow C_p^*$ reduction by gauging with liquid C_p values were published elsewhere.[18] Ferry's shear data in the frequency range from 130 to 1.6×10^4 rad/s (reported for comparison) were obtained for a fractionated PnOMA sample with M_w of 3620k.[19,20] The details of the poly(*n*-butyl methacrylate) PnBMA experiments, also reported for comparison, are published in refs 3 and 9.

III. Results

The HCS data for PnOMA indicate a crossover from a conventional ΔC_p step at low frequencies to a bend with $\Delta C_p \rightarrow 0$ in the $\alpha\beta$ splitting region (Figure 2). A small ΔC_p step is also reflected by the DSC trace for a heating rate of $T = 10$ K/min, corresponding to an effective frequency of about 1 mHz. The peaks in the imaginary part C_p'' ($\omega = 1256$ and 12560 rad/s) have a large width, and a temperature dispersion of $\delta T \approx 15$ K was obtained from a Gaussian fit. Although large $C_p''(T)$ peaks are also obtained for the high-frequency isochrones ($\omega =$ const curves), C_p'' tends to zero for $T >$ +40 °C. This corresponds to the zero dispersion of the real-part C_p' curves for $T >$ +40 °C.

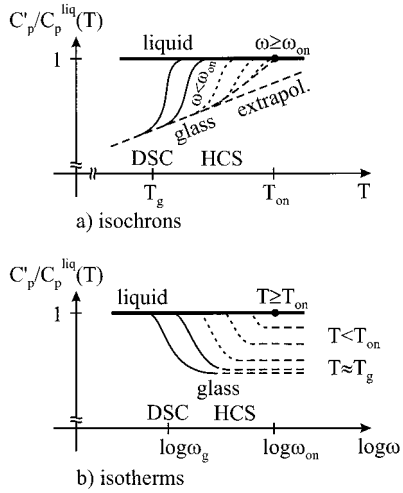

Figure 3. Diagrams schematically showing the reduced C_p' isotherms ($T =$ const (a)) and isochrones ($\omega =$ const (b)) near the onset. C_p^{liq} = the equilibrium C_p of the liquid. Possible small $\Delta C_p > 0$ steps for $T > T_{on}$ are neglected.[32]

The general behavior of the $C_p'(T,\omega)$ surface in the "below-splitting" region as obtained from HCS experiments for "near-onset" polymers (i.e., polymers with a glass transition temperature near the splitting region) is shown in Figure 3.[8,21,22] We find an α onset in the splitting region where the isothermal relaxation strength $\Delta C_p'(T)$ tends linearly to zero.[23,24] The lower part of Figure 3 schematically shows the corresponding C_p' isotherms as a function of log ω; the upper one shows the C_p' isochrones as a function of temperature T. The corresponding $C_p''(\omega, T)$ surface has peaks with decreasing peak height. The experimental HCS data for PnOMA correspond to model simulations of isothermal steps/peaks with a linear ΔC_p onset at $T_{on} = 30 \pm 5$ °C. The onset temperature was calculated from the $\Delta C_p = 0$ intersection of the extrapolated liquid and glass tangents on the $C_p'(T)$ isochrones. The onset frequency, $\log(\omega_{on}/\text{rad}\cdot\text{s}^{-1}) = 5.5 \pm 1$, was obtained after transferring the C_p'' peak maximum frequencies to an Arrhenius diagram (Figure 5, below) and extrapolating to $T \rightarrow T_{on}$.

We observed high-temperature tails for $T_{on} < T < +40$ °C of the C_p^* dispersion zone (Figure 2). They are near the resolution limit of our HCS device. A continuation of the calorimetric dispersion with $\Delta C_p/C_p \approx$ a few percent cannot, therefore, be excluded above the onset, i.e., for the high-temperature *a* process.[32]

An onset estimation from DSC is difficult for PnOMA, because ΔC_p is small, because the DSC trace is influenced by structural relaxation, and because the effective DSC frequency (≈1 mHz) is too far below HCS and the onset for a sure extrapolation (see also ref 7).

Both HCS and DSC data yield a large $(dC_p^{glass}/dT \approx 7.5 \times 10^{-3}$ J/(gK^2)) slope on the glass side (HCS in the equilibrium glass zone, and DSC in the non-equilibrium glass state). This is about twice the liquid slope from DSC, $dC_p^{liquid}/dT \approx 4.2 \times 10^{-3}$ J/(gK^2), and may be explained by a loosening of the compact glass configuration when the onset is approached. This configuration is "dynamically tested" by HCS by the high-frequency mobility in the glass zone.

The dielectric ϵ'' loss peak isotherms for PnOMA have a temperature shift of about 20 K/decade (Figure 4). There is no dramatic change of the overall dielectric intensity $\Delta\epsilon$ near the calorimetric onset temperature T_{on} ($\Delta\epsilon$ being proportional to the area of the ϵ'' peak over

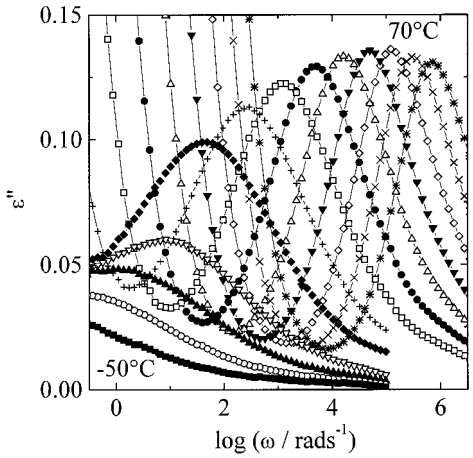

Figure 4. Dielectric loss ϵ'' of PnOMA as a function of frequency for different temperatures: (*) 70 °C; (×) 60 °C; (◇) 50 °C; (▼) 40 °C; (△) 30 °C; (●) 20 °C; (□) 10 °C; (+) 0 °C; (◆) −10 °C; (▽) −20 °C; (▲) −30 °C; (○) −40 °C; (■) −50 °C.

log ω). This is remarkable since ΔC_p steeply tends to zero at the onset (cf. refs 8 and 22) for other substances with such a behavior. As mentioned above, the reason for this difference between dielectric and HCS relaxation strength is probably that ΔC_p, being the retardation intensity of the entropy compliance, is only sensitive to *cooperative* molecular motions (i.e., only to α and not to β) whereas $\Delta\epsilon$ is sensitive to both, cooperative α and local β motions.

The separation of $\Delta\epsilon$ in $\Delta\epsilon_\alpha + \Delta\epsilon_\beta$ below the onset is impossible with only our PnOMA data. A fit of the isothermal data by a superposition of two Havriliak−Negami functions or stretched exponential decays is too delicate, because the frequency window of the equilibrium experiments is too restricted by freezing in.

A simple procedure was applied to improve the interpretation of dielectric data: The log $\omega - T$ pairs of the ϵ'' peak maxima and of both $\epsilon''_{max}/2$ = half-values of the peak wings are transferred to the Arrhenius diagram in Figure 5. The $\alpha\beta$ splitting in the dielectric data is then indicated by a pronounced broadening of the half-width interval below the calorimetric onset temperature T_{on} (inset Figure 5). The broadening mainly results from the low-frequency wing. The corresponding curve for this wing in Figure 5 is WLF-shaped and thus indicates the unresolved cooperative α relaxation. The high-frequency half-width line is Arrhenius like and indicates the β relaxation. The curve for the maxima of the whole dielectric loss peak (■ for $T > T_{on}$, □ for $T < T_{on}$) is only slightly curved below T_{on}, e.g., behaves more similar to the high-frequency half-width line or β relaxation. This indicates a low α intensity $\Delta\epsilon_\alpha$ in the splitting region compared to the β relaxation strength $\Delta\epsilon_\beta$. Such a behavior was expected from the systematic shift of the splitting region in the poly(*n*-alkyl methacrylate) series to lower frequencies for increasing side chain lengths, caused by internal plasticization.[9,25]

To find a clear separation of α and β we would have to measure at very low frequencies or to apply (moderate[26]) pressure. A quantitative evaluation of the dielectric dispersion should also pay attention to the conductivity term at low frequency (Figure 4).

The dynamic shear compliance data ($J^*(\omega,T) = J' - iJ''$) are analyzed according to the inset of Figure 1. The width of the Rouse-like region *R* with similar slopes for the real and imaginary parts, d log J'/d log $\omega \approx$ d log J''/d log ω, is defined by the two isothermal $J' = J''$ intersections. The wide frequency window accessible by

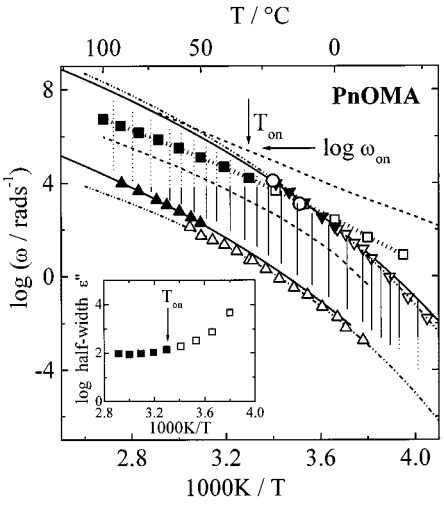

Figure 5. Arrhenius diagram for poly(*n*-octyl methacrylate) with the dielectric loss maxima above (■) and below (□) the HCS onset temperature, T_{on}, the upper (▽, ▼) and lower (△, ▲) frequency limit of the Rouse region *R*, and the $(\rho\kappa C_p)''$ maxima from HCS (○). The limits of the Rouse region were determined from shear data by Ferry[19,20] (solid triangles) and our own shear measurements (open triangles). The solid lines are WLF curves (Table 1) calculated from the shift factors by Ferry. The dashed−dotted lines are WLF fits to our upper and lower Rouse limits, and the dotted line is the fit to the dielectric loss maxima. The dashed line indicate the half-maximum values in dielectric loss. The inset shows the dielectric half-width as a function of reciprocal temperature.

the combination of the RDA II and DSR instruments allows us to determine both intersections directly from isotherms in the temperature region from −10 to 0 °C. The logarithmic width was $\Delta \log \omega \approx 4.0 \pm 0.2$, and the steepest slopes were −d log J'/d log $\omega = 0.75$ and −d log J''/d log $\omega = 0.70$. These shear exponents are larger than expected for Rouse modes (0.50). The difference is interpreted as a hydrodynamic effect (Rouse−Zimm modes) of the many CH_2 groups from the long octyl part of the side groups, forming, so to speak, a solvent for the backbone chains. The Ferry data, obtained for higher frequencies (kilohertz range) but in a smaller frequency window, show the two Rouse intersections only in the master curve.[19]

The upper intersections of the two data sets (▼, ▽) are on the same curve in an Arrhenius diagram, whereas the lower intersections show a small difference (0.4 decades) between Ferry's (▲) and our data (△, Figure 5). This difference belongs to the low-mobility Rouse limit, i.e., to large lengths of order the entanglement spacing. This limit is not important for the beyond-onset extrapolation described below, mainly based on the high-frequency Rouse limit.

Finally, all intersection frequency−temperature pairs of the shear experiments are transferred to the Arrhenius diagram (Figure 5). The Rouse-like shear modes are indicated by vertical lines: full if they are in the experimental frequency window and dotted for the range of a reasonable master-curve extrapolation. The trace of the dielectric loss maxima (squares) intersects the upper limit of the Rouse region at a temperature near the calorimetric α onset temperature T_{on}. This observation will be a major point of the discussion.

IV. Discussion and Conclusion

The question if the calorimetric onset ($\Delta C_p \rightarrow 0$ for $T \rightarrow T_{on} = 30 \pm 5$ °C) is accompanied by a dielectric onset ($\Delta\epsilon_\alpha \rightarrow 0$ for $T \rightarrow T_{on}$) cannot be decided on the basis of

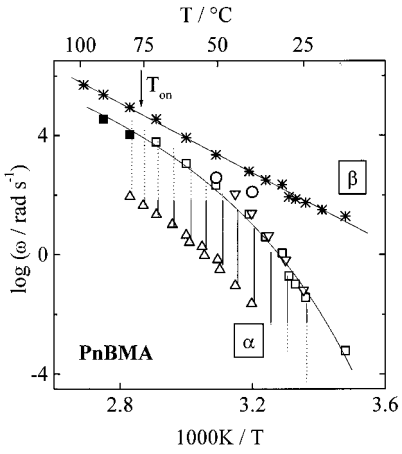

Figure 6. Arrhenius diagram for poly(*n*-butyl methacrylate)[3,9] with the dielectric loss α maxima above (■) and below (□) the HCS onset temperature, T_{on} , the dielectric loss β maxima (*), the upper (▽) and lower (△) frequency limit of the Rouse region *R*, and the $(\rho\kappa C_p)''$ maxima from HCS (○). The solid lines are WLF and Arrhenius fits to the dielectric α and β maxima.

Table 1. WLF parameters for PnOMA[a]

	log(Ω/rad s^{-1})	*B*	T_∞ /K
R (Δ)	8.8	1038	175
R (▲) (Ferry)	11.8	1653	149
R (▽)	15.5	1543	158
R (▼) (Ferry)	15.5	1653	148
ϵ''_{max} [b]	13.8	1860	109
uncertainty	±1.0	±100	±10

[a] WLF equation used: $\log \omega = \log \Omega - B/(T - T_\infty)$. [b] −20...100 °C

only our PnOMA experiments. Such a dielectric onset, however, was explicitly observed in related substances: PnBMA[9,27] PEMA,[9] random copolymers P(n-PrMA-*stat*-nPeMA).[28] and P(nBMA-*stat*-S)[22] with E = ethyl, Pr = propyl, Pe = pentyl, and S = styrene. The dielectric properties for PnOMA are very similar to those of these substances at higher temperatures. We expect, therefore, a dielectric onset also for PnOMA, although it cannot unambiguously be determined in the small remaining frequency window between ω_{on} and vitrification.

For comparison, the dielectric splitting analysis for PnBMA is illustrated in Figure 6[9] with similar symbols as in Figure 5 for PnOMA. T_{on} means here the calorimetric α onset; the dielectric α onset for PnBMA has a higher temperature and starts about one decade below the local process (*). *Below the onset the dielectric* α *trace* (□) *coincides with the upper Rouse limit* (▽). The dielectric β trace is well above the ▽ trace there. A similar but less detailed splitting scenario is indicated by Figure 5 for PnOMA. The trend to an intersection of the dielectric trace with the upper limit of the Rouse-like region near T_{on} is common for both polymers.

The advantage of the PnOMA diagram is that Rouse modes were measured by Ferry at higher frequencies, so that a definite comparison between extrapolated shear data and dielectric data beyond the onset can be made. We see that *the dielectric trace of local molecular motions intersects the upper Rouse limit below (but near) the onset and tends, above the onset temperature, to the middle of the Rouse-like region.* The WLF limiting frequency Ω for the dielectric data is about in the middle of the Rouse-limit Ω's, obtained from separated WLF fits (Table 1). We have never found such a tendency in polymers far below the $\alpha\beta$ splitting. Usually, nearly parallel traces for the limits of the Rouse-like region and the dielectric loss maximum are obtained there, without indications to an intersection.[29]

The WLF equation used here is $\log \omega = \log \Omega - B/(T - T_\infty)$. The complete set of WLF parameters for PnOMA is given in Table 1.

The different frequency positions of dielectric signals relative to the Rouse zone for $T < T_{on}$ and $T > T_{on}$ are interpreted by different dipole compensation mechanisms. Below the onset, $T < T_{on}$, the maximal α dipole fluctuation corresponds to the cooperative α glass transition, as indicated by the coincidence of the α dielectric with the HCS trace (Figure 6). The local β relaxation is well separated from the main transition α (Figures 5 and 6). Above the onset, $T > T_{on}$, where the α cooperativity from HCS is expected to be absent or small, the maximal fluctuation of local dipoles corresponds to a certain average Rouse−Zimm mode between the entanglements (Figure 5). This means for our PnOMA sample that Rouse−Zimm modes cannot completely compensate for the monomeric dipoles. Such a zero compensation was, however, expected since the dipole moments are connected with the carboxyl groups, giving no or only a small dipole component along the chains.

This dipole compensation mechanism, the zero or small calorimetric activity expected above the onset, and the low curvature of the high-temperature part of all traces in the Arrhenius diagram seem to indicate that the main transition in PnOMA above T_{on} is characterized by modified Rouse−Zimm modes with no or only a small molecular α cooperativity.

This conjecture will be illustrated by two remarks.

(i) Molecular mobility is of course needed for Rouse−Zimm modes of the chain backbones. It is still an open question if such a mobility can only be generated by a polyethylene-like (PE) glass transition of the CH_2 groups at higher frequencies. The corresponding γ relaxation of PE at 30 °C is at $\log \omega \approx 9.5 \pm 1$, i.e., about 4 decades higher than $\log \omega_{on}$(PnOMA). Such an additional high-frequency dispersion zone was really observed in poly(*n*-lauryl methacrylate).[30] Indications for such an additional relaxation process can also be found in the shear curves for poly(*n*-pentyl methacrylate) and poly(*n*-hexyl methacrylate).[31]

(ii) It would be of great importance if our high-temperature behavior can be generalized to other polymers above the splitting region. The splitting regions for polymers such as polystyrene, poly(vinyl acetate), or poly(vinyl chloride) are in the log ω region between 7 and 10. Considering too small free volume as the reason for a cooperativity below the onset, we may speculate as follows: Since we have enough free volume above the onset, the monomeric units have a high mobility, also without a CH_2 solvent. There is no need for a specific molecular α cooperativity there, so that the main transition of polymers at high frequencies is reduced to Rouse-like modes.

In summary, our experiments indicate a cooperativity onset $\Delta C_p \rightarrow 0$ ($\Delta C_p/C_p <$ a few percent) in the $\alpha\beta$ splitting region of PnOMA. This means that the Rouse−Zimm-like modes above the onset are probably not accompanied by a specific molecular α cooperativity of the short, high-frequency modes as for polymers far below the $\alpha\beta$ splitting region. The application of the time−temperature superposition from below to above the splitting can, therefore, not be recommended for an

estimation of the high-temperature *a* process above the splitting.

Acknowledgment. We thank Dr. W. Steffen (MPI-P Mainz) for providing the PnOMA sample, and the Deutsche Forschungsgemeinschaft DFG and the Fonds Chemische Industrie FCI for financial support.

References and Notes

(1) Grosch, K. A. *Proc. R. Soc.* **1963**, *A274* , 21.
(2) Ngai, K. L.; Plazek, D. J. *Rubber Chem. Technol.* **1995**, *68*, 376.
(3) Donth, E.; Beiner, M.; Reissig, S.; Korus, J.; Garwe, F.; Vieweg, S.; Kahle, S.; Hempel, E.; Schröter, K. *Macromolecules* **1996**, *29*, 6589.
(4) Reissig, S.; Beiner, M.; Vieweg, S.; Schröter, K.; Donth, E. *Macromolecules* **1996**, *29*, 3996.
(5) Santangelo, P. G.; Ngai, K. L.; Roland, C. M. *Macromolecules* **1993**, *26*, 2682. Ngai, K. L.; Plazek, D. J.; Deo, S. S. *Macromolecules* **1987**, *20*, 3047.
(6) Richter, D.; Willner, L.; Zirkel, A.; Farago, B.; Fetters, L. J.; Huang, J. S. *Phys. Rev. Lett.* **1993**, *71*, 4158.
(7) Hempel, E.; Beiner, M.; Renner, T.; Donth, E. *Acta Polym.* **1996**, *47*, 525.
(8) Donth, E.; Kahle, S.; Korus, J.; Beiner, M. *J. Phys. I (Fr.)* **1997**, *7*, 581.
(9) Garwe, F.; Schönhals, A.; Lockwenz, H.; Beiner, M.; Schröter, K.; Donth, E. *Macromolecules* **1996**, *29*, 247.
(10) Casalini, R.; Fioretto, D.; Livi, A.; Lucchesi, M.; Rolla, P. A. *Phys. Rev. B* **1997**, *56*, 3016.
(11) Corezzi, S.; Capaccioli, S.; Gallone, G.; Livi, A.; Rolla, P. A. *J. Phys.: Condens. Matter* **1997**, *9*, 6199.
(12) Arbe, A.; Richter, D.; Colmenero, J.; Farago, B. *Phys. Rev. E* **1996**, *54*, 3853.
(13) Stickel, F.; Fischer, E. W.; Richert, R. *J. Chem. Phys.* **1995**, *102*, 6251.
(14) Stickel, F.; Fischer, E. W.; Richert, R. *J. Chem. Phys.* **1996**, *104*, 2043.
(15) Stickel, F. Thesis, Universität Mainz, Shaker, Aachen, 1995.
(16) Hansen, C.; Stickel, F.; Berger, T.; Richert, R.; Fischer, E. W. *J. Chem. Phys.* **1997**, *107*, 1086.
(17) Birge, N. O.; Nagel, S. R. *Phys. Rev. Lett.* **1985**, *54*, 2674.
(18) Korus, J.; Beiner, M.; Busse, K.; Kahle, S.; Donth, E. *Thermochim. Acta*, in press.
(19) Dannhauser, W.; Child, W. C.; Ferry, J. D. *J. Colloid Sci.* **1958**, *13*, 103.
(20) Berge, J. W.; Saunders, P. R.; Ferry, J. D. *J. Colloid Sci.* **1959**, *14*, 135.
(21) Donth, E. *J. Polym. Sci., Polym. Phys. Ed.* **1996**, *34*, 2881.
(22) Kahle, S.; Korus, J.; Hempel, E.; Unger, R.; Höring, S.; Schröter, K.; Donth, E. *Macromolecules* **1997**, *30*, 7214.
(23) Such a linear behavior is also found by numerical simulations based on a modified Fredrickson model with stochastical energy barriers for the local processes. For details see: Schulz, M.; Donth E. *J. Non-Cryst. Solids* **1994**, *168*, 186.
(24) Korus, J.; Hempel, E.; Beiner, M.; Kahle, S.; Donth, E. *Acta Polym.* **1997**, *48*, 369.
(25) Heijboer, J. In: *Physics of Non-crystalline Solids*; Proceedings International Conference Delft, July 1964; Prins, J. A., Ed.; North-Holland, Amsterdam, 1965; p 231.
(26) Sasabe, H.; Saito, S. *J. Polym. Sci., Polym. Phys. Ed.* **1968**, *6*, 1401.
(27) Garwe, F.; Schönhals, A.; Beiner, M.; Schröter, K.; Donth, E. *J. Phys.: Condens. Matter* **1994**, *6*, 6941.
(28) Zeeb, S.; Höring, S.; Garwe, F.; Beiner, M.; Hempel, E.; Schönhals, A.; Schröter, K.; Donth, E. *Polymer* **1997**, *38*, 4011.
(29) Beiner, M. Thesis, Universität Halle, 1995.
(30) Floudas, G.; Placke, P.; Stepanek, P.; Brown, W.; Fytas, G.; Ngai, K. L. *Macromolecules* **1995**, *28*, 6799.
(31) Heijboer, J. In *Static and Dynamic Properties of the Polymeric Solid State*; Pethrick, R. A., Richards, R. W., Eds.; NATO Advanced Study Institutes Series Vol. 94; Reidel: Dordrecht, The Netherlands 1982; p 197.
(32) Note added in proof: New HCS experiments in our lab on poly(*n*-hexyl methacrylate) show that the high temperature *a* process is weakly calorimetrically active: We find nearly constant values for $\Delta C_p \approx 0.11 \pm 0.03$ J/g·K and $\delta T \approx 19 \pm 3$ K above the onset. Below the onset a linear increase of ΔC_p with $T_{on} - T$ was observed in random copolymers poly(styrene-*stat*-nBMA).[22] This is interpreted as an additional indication that the main transition consists of two distinct parts: a weakly cooperative high temperature process *a* above and the cooperative glass transition α below the onset.

MA961704P